Orientation of the Eruption Fissures Controlled by a Shallow Magma Chamber in Miyakejima

Nobuo Geshi* and Teruki Oikawa

Institute of Earthquake and Volcano Geology, Geological Survey of Japan, National Institute of Advanced Industrial Science and Technology (AIST), Tsukuba, Japan

Orientation of the eruption fissures and composition of the lavas of the Miyakejima volcano is indicative of the competitive processes of the regional tectonic stress and the local stress generated by the activity of a magma plumbing system beneath the volcano. We examined the distributions and magmatic compositions of 23 fissures that formed within the last 2800 years, based on a field survey and a new dataset of ^{14}C ages. The dominant orientation of the eruption fissures in the central portion of the volcano was found to be NE-SW, which is perpendicular to the direction of regional maximum horizontal compressive stress (σ_{Hmax}). Magmas that show evidence of mixing between basaltic and andesitic compositions erupted mainly from the eruption fissures with a higher offset angle from the regional σ_{Hmax} direction. The presence of a dike pattern perpendicular to the direction of maximum compression σ_{Hmax} is an unusual and uncommon feature in volcanoes. Here we investigate the conditions possibly controlling this unexpected dike pattern. The distribution and magmatic compositions of the eruption fissures in Miyakejima volcano highlight the tectonic influence of shallow magma chamber on the development of feeder dikes in a composite volcano. The presence of a shallow dike-shaped magma chamber controls the eccentric distribution of the eruption fissures perpendicular to the present direction of σ_{Hmax}. The injection of basaltic magma into the shallow andesitic magma chamber caused the temporal rise of internal magmatic pressure in the shallow magma chamber which elongates in NE-SW direction. Dikes extending from the andesitic magma chamber intrude along the local stress field which is generated by the internal excess pressure of the andesitic magma chamber. As the result, the eruption fissures trend parallel to the elongation direction of the shallow magma chamber. Some basaltic dikes from the deep-seated magma chamber reach the ground surface without intersection with the andesitic magma chamber. These basaltic dikes develop parallel to the regional compressive stress in NW-SE direction. The patterns of the eruption fissures can be modified in the future as was observed in the case of the destruction of the shallow magma chamber during the 2000 AD eruption.

Keywords: fissure eruption, feeder dike, magma chamber, local stress, Miyakejima

INTRODUCTION

Propagation of a dike is controlled by the stress field in its host rock; the orientation of a dike is basically parallel to the maximum compressive axis ($\sigma 1$) and perpendicular to the minimum compressive axis ($\sigma 3$). Therefore, the orientation of dikes has been used as an indicator of the stress field in volcanic fields (Nakamura, 1977; Yamaji and Sato, 2011). Dikes will be oriented parallel to the maximum stress axis in a homogeneous stress field. However, the distribution of dikes and eruption fissures in volcanoes display radial, circumferential, and curvature patterns reflecting the local stress in the volcanic edifice (e.g., Chadwick and Howard, 1991). Local disturbances in the stress field of a volcano are caused by the prominent topography of a volcanic edifice (e.g., Tibaldi et al., 2014), flank instability (e.g., Walter et al., 2005), unloading by collapse (Corbi et al., 2015), active faults near the volcanic system (e.g., Seebeck and Nicol, 2009), mechanical heterogeneity in the volcanic edifice and basement (e.g., Letourneur et al., 2008), and the magmatic activity within the volcano (e.g., Chadwick and Dieterich, 1995; Takada, 1997). Recent observations of the dike intrusion events reveal that the stress field in the host rock is affected by the emplacement of intrusions, and consequently feedbacks to the growth of the next dikes (e.g., Bagnardi et al., 2013; Falsaperla and Neri, 2015).

The local pressure source within a volcano is one of the major causes of a local disturbance in the stress field within the volcano (Gudmundsson, 2006). Magma injection into a local magma reservoir results in a rise of magma pressure, and it consequently has a strong influence on the distribution pattern of an eruptive fissure (e.g., Tibaldi, 2015 and the references therein). Therefore, utilizing the knowledge of local disturbances in a stress field within a volcano, we can predict the distribution pattern of fissure eruptions.

Predicting the distribution pattern of flank fissure eruptions is not only pertinent to volcanology but is also of critical importance to hazard management. As the site and orientation of fissure eruptions are controlled by the orientation and propagation direction of the feeder dikes, understanding of the stress field within a volcano and the propagation direction of feeder dikes are crucial to evaluating the risk of flank fissure eruptions (e.g., Gudmundsson, 2006). Flank fissure eruptions are one of the major causes of volcanic disasters (Cappello et al., 2015).

The distribution of the flank fissure eruptions in Miyakejima Island is indicative of the competitive processes of the regional tectonic stress and the local stress generated by the activity of a magma plumbing system beneath the volcano (Nakamura, 1977). The development of a rift zone perpendicular to the regional horizontal compressive axis (σ_{Hmax}) provides a good example of the role of a local stress field within the volcanic edifice on the distribution of the eruption fissures. A combination of the inferences made from geological and petrological investigations and the observations from a recent caldera collapse event reveal the influence of shallow magma chambers on the development of eruption fissures. Here, we examined the distribution patterns of recent eruption fissures, with a new dataset of ^{14}C ages and petrological analysis to reveal the influence of a shallow magma chamber.

BACKGROUND OF MIYAKEJIMA

Tectonic Setting

The northernmost part of the Izu-Bonin volcanic arc, including Miyakejima, is compressed in the NW-SE direction owing to the subduction of the Philippine Sea Plate to the Eurasian Plate (**Figure 1A**). The orientations of several volcanic chains in the northernmost part of the Izu-Bonin volcanic arc are consistent with the NW-SE compression in this area (Nakamura, 1977). Focal mechanisms of the earthquakes in the vicinity of Miyakejima also indicate that the σ_{Hmax} is aligned in the NW-SE direction and σ_{Hmin} in the NE-SW direction (Nishimura, 2011). Orientations of volcanic fissures in the Izu-Tobu monogenic volcanoes, ~100 km north of Miyakejima, are predominantly NW-SE (Koyama and Umino, 1991). The Izu-Oshima volcano, ~60 km north of Miyakejima, also has volcanic chains on its flank trending in the WNW-ESE direction in the northwestern flank and in the NW-SE direction in the southeastern flank (Ishizuka et al., 2014). The Hachijojima volcano, ~100 km south of Miyakejima, has volcanic chains trending in the NW-SE direction (Ishizuka et al., 2008). A regional dike trending in the N45°W direction intruded the submarine area between Miyakejima Island and Kozushima Island during the 2000 AD eruption (**Figure 1A**: Ito and Yoshida, 2002; Yamaoka et al., 2005).

The dominant orientation of the eruption fissures in the Miyakejima volcano is, however, different from its neighboring volcanoes (Nakamura, 1977). The eruption fissures in the Miyakejima volcano are concentrated in the NE-SW direction near the summit, giving rise to a NE-SW rift zone (**Figure 1B**). The eruption fissures tend to curve to trend in the NW-SE direction in the coastal, peripheral part of the island (Nakamura, 1977; Aramaki et al., 1986).

Geology

The Miykejima volcano is a basaltic–andesitic composite volcano sitting on the Izu-Bonin volcanic arc on the Philippine Sea Plate (**Figure 1A**). Miyakejima has a conical volcanic edifice, which extends ~700 m high above sea level and ~500 m below sea level (**Figure 1B**). Four eruptions were recorded in the last 100 years, two in the northeastern flank (the 1940 and 1962 eruptions) and two in the southwestern flank (the 1983 eruption and the 2000 submarine eruption).

The development of chains of scoria cones on the flanks of the island indicates the frequent lateral fissure eruptions during the development of the volcano (Tsukui and Suzuki, 1999). Though fissure eruptions occurred throughout the history of the volcano, we focused on the fissure eruptions after the formation of Hachodaira caldera because the formation of the Hachodaira caldera is one of the key events in the development of the volcano. Phreatomagmatic eruptions during the caldera formation produced the Hachodaira ash layer, which provides good key bed in all part of the island. Our new ^{14}C data indicate that the Hachodaira caldera was formed at 2700–2800 years ago.
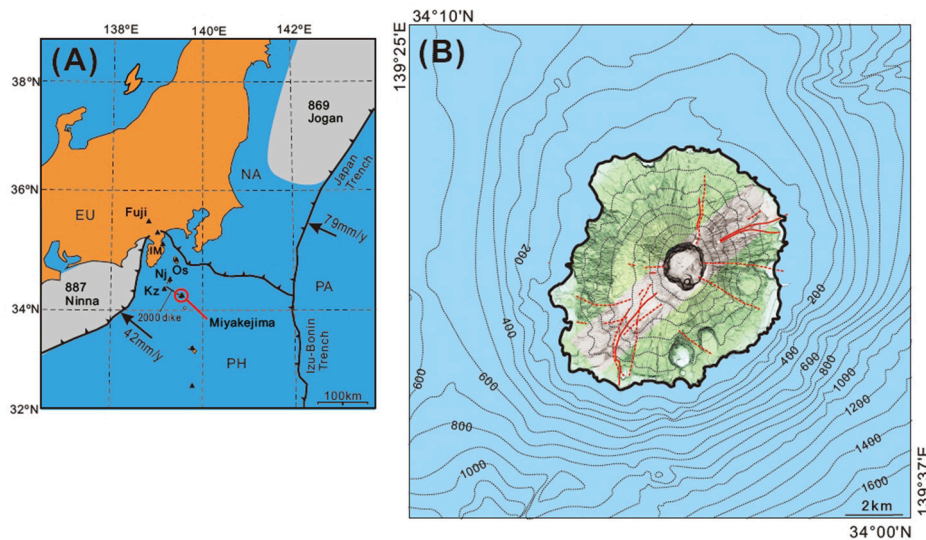
FIGURE 1 | (A) Tectonic setting of the Miyakejima Island. PH, Philippine Sea Plate; PA, Pacific Plate; NA, North America Plate; EU, Eurasia Plate Arrows indicate the direction and speed of the subduction at the trench. Solid triangles show the location of active volcanoes. IM, Izu-Tobu Monogenetic Volcanoes; Os, Izu-Oshima; Nj, Niijima; Kz, Kozushima. Gray areas show the approximate source area of the 869AD Jogan earthquake and the 887AD Ninna-Nankai earthquake. (B) Distribution of the eruption fissures. Solid red lines show the eruption fissure in the nineteenth and twentieth centuries. Historical records confirm their ages. Broken red lines show the eruption fissures younger than the seventh century. Their ages are suggested by the ^{14}C age. The shadowed area shows the approximate area of the NE-SW rift zone. Counters are 100 m interval.

A new collapse caldera, which is 1.7 km across, was formed at the summit during the 2000 AD eruption due to the draining of the shallow andesitic magma chamber through a large lateral intrusion (Geshi et al., 2002). Temporal changes of the juvenile material during the eruption show that the dike intrusion to the northwest of the island withdrew andesitic magma from a shallow chamber, which was then replaced by basaltic magma in the later stage of eruption (Geshi et al., 2002).

Magma Plumbing System

The magmas that erupted from Miyakejima volcano within the last 2800 years have been basaltic to andesitic in composition, with whole-rock SiO_2 contents ranging from 50 to 62 wt% (**Figure 2**). The disequilibrium mineral assemblage and the wide and linear variations of the whole-rock composition of the basaltic-andesite of Miyakejima indicate mixing between the basaltic and andesitic end components (Amma-Miyasaka and Nakagawa, 2003; Kuritani et al., 2003). Judging by the narrow diffusion texture at the rim of the olivine phenocrysts, magma mixing occurred just before the eruption (Niihori et al., 2003).
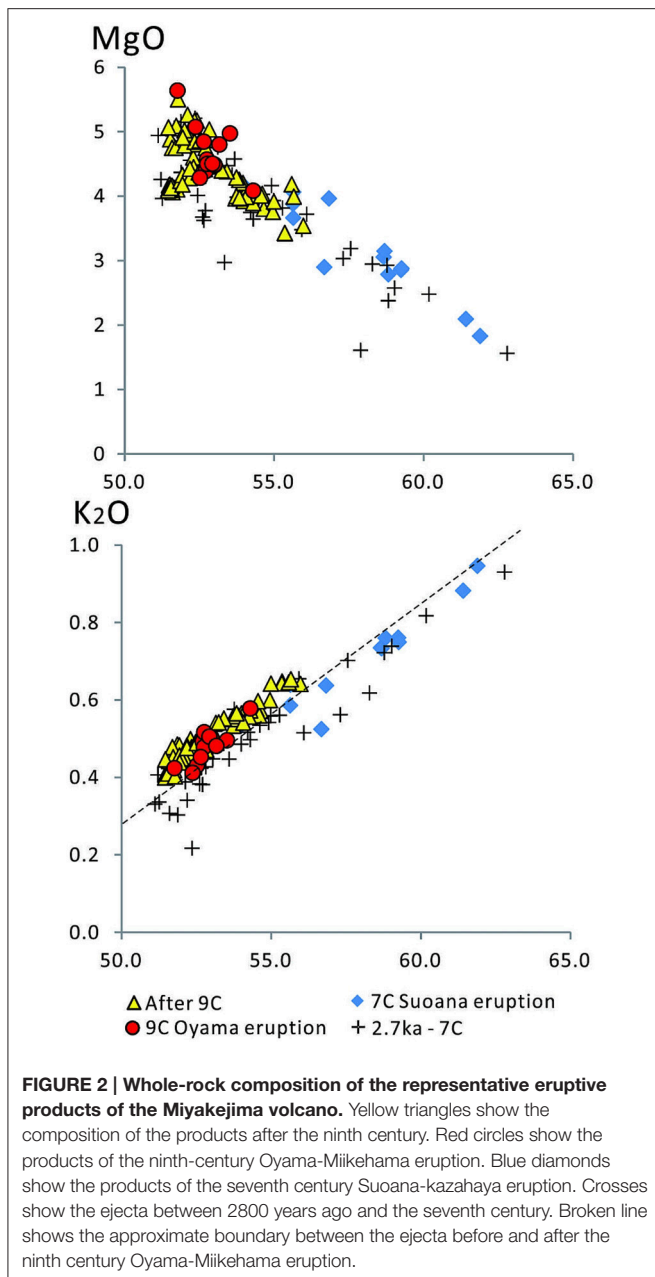
The basaltic magma, which is fed from the deeper chamber, has the whole-rock SiO_2 content of ∼50–51 wt%. Equilibrium relationships between minerals and the groundmass suggest that the less-fractionated magmas with basaltic compositions are stored in a magma chamber at around ∼200 MPa. Whereas the fractionating magmas with andesitic compositions are stored at a shallower depth at around ∼100 MPa (Kuritani et al., 2003; Amma-Miyasaka et al., 2005). These pressures correspond to depth of ∼10 km for the basaltic magma and ∼5 km for the andesitic magma, respectively.

RECONSTRUCTION OF ERUPTION FISSURES

Distribution and Age of the Eruption Fissures

The distribution and ages of the eruption fissures in Miyakejima were re-examined to reveal the temporal distribution patterns of the flank fissure eruptions in the volcano. The locations and orientations of the eruption fissures were confirmed, based on aerial photographs, a digital elevation model (5 m grid provided by the Geospatial Information Authority of Japan), and our field survey. The ages of each of the eruption fissures were determined by both the stratigraphic relationships of the tephra layers and the ^{14}C dating of the carbonized plant fragments at the base of the tephra layer.

In this study, we focus on the eruption fissures younger than the 2.7–2.8 ka caldera-forming event. We confirmed 23 fissure eruptions in this period (**Table 1**). Among them, sixteen fissure eruptions were identified as being younger than the seventh century Suoana-Kazahaya eruption (**Figure 3** and **Table 1**). The eruption fissures younger than the seventh century are mainly distributed in the NE-SW rift zone. Since the seventh century, four fissure eruptions occurred in the northeastern sector of the volcano, and ten occurred in the southwestern sector of the volcano. Two fissure eruptions (Ninth century and sixteenth century) occurred in the eastern flank. Though the exposure of the eruption fissures before the seventh century is limited owing to the coverage by the younger deposits, we also confirmed the locations and ages of six fissure eruptions between 2.5 ka and the seventh century (**Table 1**). Among the six eruptions,

FIGURE 2 | Whole-rock composition of the representative eruptive products of the Miyakejima volcano. Yellow triangles show the composition of the products after the ninth century. Red circles show the products of the ninth-century Oyama-Miikehama eruption. Blue diamonds show the products of the seventh century Suoana-kazahaya eruption. Crosses show the ejecta between 2800 years ago and the seventh century. Broken line shows the approximate boundary between the ejecta before and after the ninth century Oyama-Miikehama eruption.

only two (Hatchodaira and Daihannyayama) occurred in the NE-SW rift.

Here, we introduce the "offset angle" of eruption fissures to evaluate the direction of the eruption fissures (**Figure 4A**). Offset angle is defined as the angle between the strike of the eruption fissure at the near side and the direction of the maximum horizontal compressive stress (σ_{Hmax}). The offset angle varies from 0° (parallel to the σ_{Hmax}) to 90° (perpendicular to the σ_{Hmax}). The direction of σ_{Hmax} is assumed to be N135°E, based on the strike of the regional dike intruded during the 2000 AD eruption (Ito and Yoshida, 2002; Yamaoka et al., 2005). The eruption fissures in the NE-SW rift zone have high offset angles ranging from 40° to 90°.

Magma Composition

The relationship between the orientation of eruption fissures and the composition of magma is investigated. We analyzed the whole-rock compositions of lavas and/or scoria of the fissure eruptions within the last ~2800 years. Whole-rock compositions of the erupted products form a linear compositional trend (**Figure 2**). A detailed examination indicated that the whole-rock K_2O contents of the products after the ninth century are slightly higher than that of the products between 2.8 ka and the seventh century (**Figure 2**).

Whole-rock SiO_2 contents of the lavas from the flank eruptions show wider variations with the increase of the offset angle of the eruption fissure (**Figure 4B**). Basaltic magmas (SiO_2 ~51 wt%) erupted in all directions, whereas the magmas with higher SiO_2 content erupted from the fissures with a higher offset angle (**Figure 4B**). The eruption fissures with offset angles less than 30° erupted basaltic andesite with a <53 wt% of whole-rock SiO_2 content. Andesite with SiO_2 >56 wt% was erupted from two fissures; the seventh century fissure in the northern flank with an offset angle of ~60° and the 2.7–2.8 ka eruption from the southern flank with an offset angle of ~85°.

DISCUSSION

A combined analysis of the location, age, and magmatic composition of the lavas of the eruption fissures in Miyakejima revealed the following facts: (i) The eruption fissures with higher offset angles from the regional compressive direction occurred within the last ~2800 years and formed the NE-SW rift, and (ii) Magmas with significant evidence of magma mixing erupted mainly from the eruption fissures with larger offset angles.

The limited distribution of hybrid magma in the NE-SW rift zone confirms the presence of an andesitic magma chamber beneath the NE-SW rift zone in the summit area. Several previous works on the petrological analysis of Miyakejima (Amma-Miyasaka and Nakagawa, 2003; Kuritani et al., 2003; Niihori et al., 2003; Amma-Miyasaka et al., 2005) show that the magmas that erupted within the last ~2800 years are hybrid with basaltic and andesitic end-components. The mixed end components were stored in a duplicated magma chamber system consisting of a deep-seated basaltic chamber and a shallow andesitic chamber. An analysis of the volatile component concentration of the melt inclusion in the ejecta of the 2000 AD eruption indicates that the equilibrium depth of basaltic magma is ~8 km for basaltic magma and ~3–5 km for andesitic magma (Saito et al., 2005, 2010).

Geophysical and geochemical observations also support the theory of a duplex magma chamber system beneath the Miyakejima before and during the 2000 AD eruption. The existence of a deep-seated basaltic magma chamber is suggested by the presence of the inflation source at around 9.5 km below sea level prior to the eruption (Nishimura et al., 2001). The existence of a shallow magma chamber at ~3–5 km below sea level is suggested by the position of the deflation source during the 2000 eruption (Nishimura et al., 2001), the source depth of the very-long-period seismic signal (Kumagai et al., 2001; Kobayashi et al.,

TABLE 1 | Age, offset angle, and whole-rock composition of fissure eruptions.

Name of eruption	Age	14$_C$ age	Location	Offset angle	Whole-rock SiO$_2$ wt.%
Hatchodaira	2.7–2.8 ka		SW flank	45	56.1–58.8
Kanaso-minami	2.1 ka	2110 ± 30 BP	E flank	50	52.2
Tairayama	2.1 ka		NW flank	19	52.7–53.4
Tairoike	2.0 ka	1950 ± 20 BP	S flank	20	54.0
Daihannyayama	1.8 ka	>1880 ± 30 BP	NE flank	60	54.2
Anegakata	~2 ka		NW flank	10	50.0
Suoana-Kazahaya	Seventh century	1410 ± 30 yrBP, 1360 ± 20 yrBP	N flank	60	54.0–61.4
Oyama-Miikehama	Ninth century	1240 ± 20 yrBP	E-W summit-flank	50	51.8–54.3
Kamane	0.9 ka	860 ± 20 yrBP	SW flank	80	52.0
Nanto	1085 AD?	750 ± 20 yrBP	SW flank	65	55.0
Hinoyama	1154 AD?	700 ± 20 yrBP, 690 ± 20 yrBP	NE flank	85	53.7
Enokizawa	1469 AD?		W flank	40	52.6–53.2
Sonei-Bokujo			Summit	–	52.2–54.1
Benkene	1535 AD?	340 ± 20 yrBP, 380 ± 20 yrBP, 390 ± 20 yrBP	E flank	15	51.8–52.8
Jinanyama	1595 AD?	315 ± 20 yrBP, 320 ± 20 yrBP	SW flank	85	52.1–52.8
Koshiki-Imasaki	1643 AD	250 ± 20 yrBP	SW flank	70	52.2–52.9
Shinmio	1712 AD?		SW flank	85	55.0
Tatsune	1763 AD?		SW flank	90	52.2
Bunka	1811 AD		Summit?	–	
Kasaji-Kannon	1835 AD		W flank	55	56.0
1874 AD (Meiji)	1874 AD		N flank	50	51.9–54.3
1940 AD	1940 AD		NE flank and summit	80	50.8–55.7*
1962 AD	1962 AD		NE flank	80	52.2–54.7*
1983 AD	1983 AD		SW flank	85	52.5–54.7**
2000 AD	2000 AD		SW flank (submarine)	45	51.7–54.0

*Amma-Miyasaka and Nakagawa (2003), **Kuritani et al. (2003).
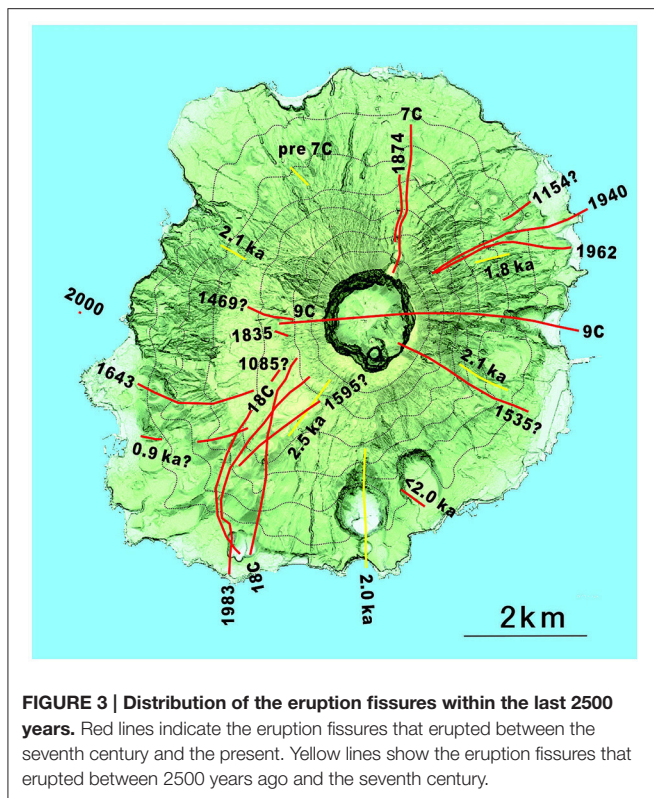Ages with "?" are not supported by the historic records.

2009), and the location of the dike injection at the initial stage of eruption (Ueda et al., 2005; Irwan et al., 2006). Source analysis of the very-long-period seismic signal and tilt change reveals the existence of a vertically aligned and NE-SW elongated ellipsoidal magma chamber at around 2.6 km beneath the south flank of the edifice (Munekane et al., 2016).

These petrological and geophysical observations indicate the existence of a duplicated magma plumbing system with a deep (~10 km) basaltic chamber and shallow (~2–5 km) andesitic magma chamber. Intermittent injections of basaltic magma into the shallow andesitic magma chamber formed hybrid magmas with higher SiO$_2$ concentrations. The injection of basaltic magma into a shallow magma chamber also caused rapid rise of internal magmatic pressure in the shallow magma chamber. This rapid increase of internal magmatic pressure may cause the dike propagation from the shallow magma chamber to feed a fissure eruption. Narrow diffusion profile observed in the titanomagnetite crystals of the andesitic ejecta suggests that the rupturing of the magma chamber and fissure eruption occurred within a few hours after the injection of basaltic magma into the andesitic system (Kuritani et al., 2003). A shallow magma chamber with a NE-SW trend and an elongated shape will form a stress field to accommodate the NE-SW trending vertical dikes above the magma chamber (**Figure 5A**). A feeder dike, which

propagated from the shallow magma chamber, reached the NE-SW rift zone and erupted magmas with a signature of magma mixing between andesite and basalt.

Development of feeder dike system controlled by a duplex magma chamber proposed for the Miyakejima's system is similar to the feeding system of the 2005 eruption of Fernandina volcano, Galapagos (Chadwick et al., 2011). Petrological evidences of the lavas support the tapping of magma from the shallow magma chamber (Chadwick et al., 2011). The path of the feeder dike followed the maximum compressive stress generated by the overpressurized sill-like chamber (Chadwick and Dieterich, 1995) and also the existence of caldera (Corbi et al., 2015) to form a circumferential fissure. Development of the circumferential inclined sheets in Fernandina is controlled by the shape of the shallow magma chamber (horizontal sill), whereas the vertical dike-like shape of the shallow chamber in Miyakejima forms preferred oriented vertical feeder dikes. Difference of the regional tectonic setting [almost isotropic horizontal stress in Fernandina (Chadwick and Dieterich, 1995) and strong horizontal differential stress in Miyakejima (Nishimura, 2011)] may control the difference of the orientation of the shallow chambers.

Development of the compressive stress field around the shallow andesitic magma chamber is limited at the time of

FIGURE 3 | Distribution of the eruption fissures within the last 2500 years. Red lines indicate the eruption fissures that erupted between the seventh century and the present. Yellow lines show the eruption fissures that erupted between 2500 years ago and the seventh century.

basaltic injection because pressure in the shallow andesitic magma chamber drops with the withdrawal of magma to the eruption fissure and/or the relaxation of the host rock surrounding the magma chamber. Some dikes from a deep-seated magma chamber could propagate directly to the ground surface and caused fissure eruptions of basaltic lavas (e.g., the 1535 eruption). In this case, the shallow magma chamber is not affected by the injection and, therefore, the magma chamber did not have any remarkable stress effect on the propagation of the basaltic dike (**Figure 5B**). Propagation of these basaltic dikes is mainly controlled by the regional stress field, and/or local stress field generated by the deep-seated basaltic magma chamber.
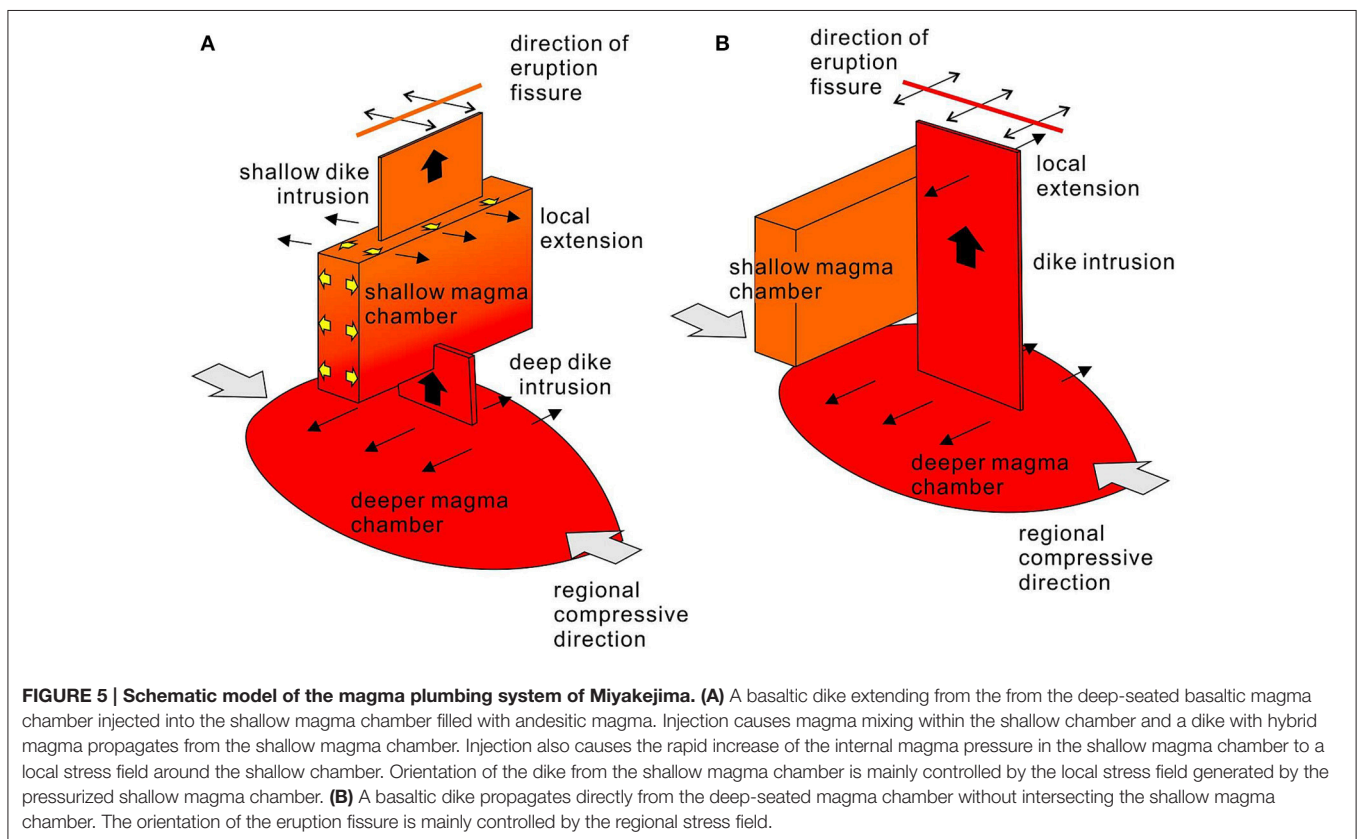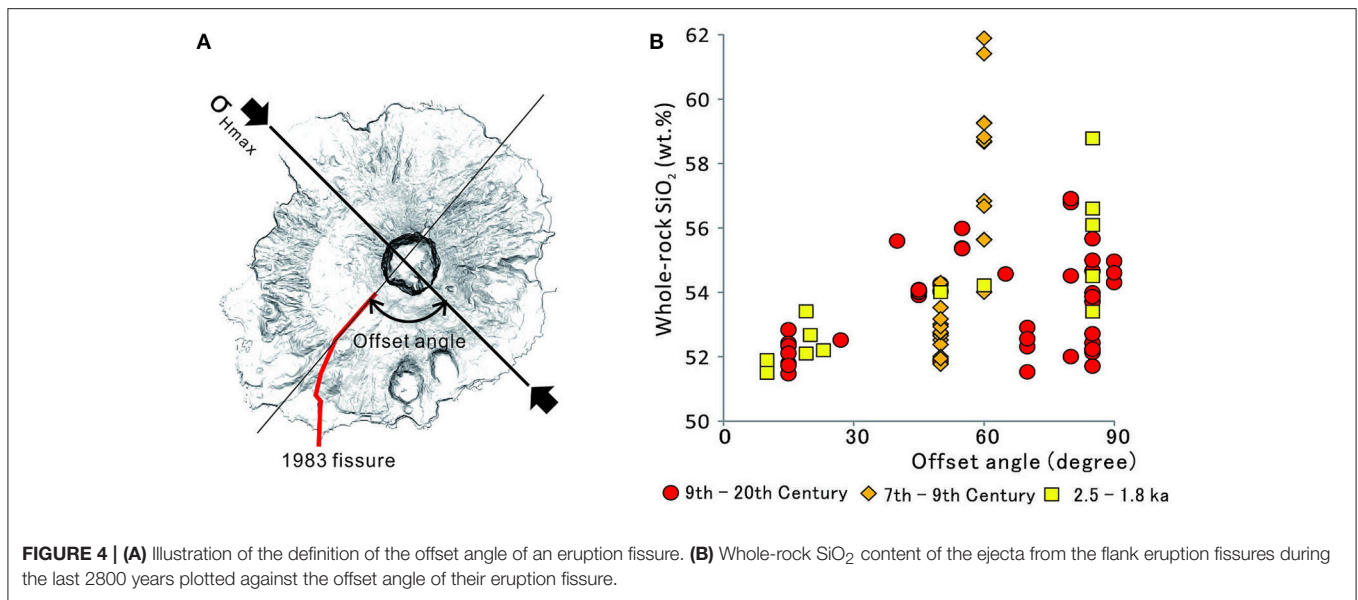
Our dataset of the ^{14}C dating shows that the development of the NE-SW rift zone became significant after the ninth century. This suggests that the shallow andesitic magma chamber was formed after the ninth century. The Oyama-Miikehama in the middle of the ninth century eruption erupted a volume of ~0.08 km^3 DRE of basaltic magma (Tsukui and Suzuki, 1999) from the summit crater and an eruption fissure ~5 km in length. The Oyama-Miikehama eruption is the largest eruption within the last ~2800 years after the formation of the Hatchodaira caldera. A part of the basaltic magma, which was intruded during this eruption, formed a secondary magma chamber at a shallow depth and produced andesitic magma with fractional crystallization. A shift from the compositional trend of the eruption products since the ninth century (**Figure 2**) suggests the formation of a new magma system at the Oyama-Miikehama eruption. The existence of a similar secondary magma chamber is also recognized in the neighboring basaltic volcanoes (e.g., source of the 1986 fissure eruption in Izu-Oshima; Nakano

and Yamamoto, 1991). NE-SW elongated shape of the shallow magma chamber may control the emplacement direction of the dikes, though the reason why the shallow magma chamber was formed perpendicular to the regional σ_{Hmax} direction is still open to debate. One of the possibilities is the disturbance of stress field by coseismic extensional deformation at the plate boundary earthquake (e.g., The 2011 Tohoku earthquake; Ozawa and Fujita, 2013). Two large trench-type earthquakes occurred in the ninth century (the 869AD Jogan Earthquake M>8.3 at Japan Trench and the 887AD Ninna-Nankai Earthquake Mw>8.6 at Nankai Trough; **Figure 1A**). These earthquakes might change the stress field from the NW-SE compressive state to the NW-SE extensive one in which a NE-SW elongated magma chamber can be formed. Tectonic disturbance is also suggested by frequent and intensive eruptions in the ninth century in the northern part of the Izu area (e.g., eruptions of Kozushima 838AD, Niijima 886AD, Mt. Fuji 864AD; Tsukui et al., 2006).

In the future, distribution pattern of the fissure eruptions in the future can change to a radial or NW-SE trend depending on the properties of the regional tectonic stress. During the caldera formation of the 2000 eruption, the shallow magma chamber of andesitic magma was emptied and collapsed (Geshi et al., 2002). Basaltic ejecta in the later stage of the eruption indicate that the shallow andesitic magma chamber was completely replaced by the basaltic magma. Therefore, the feeder dikes can intrude directly from the deep-seated basaltic magma chamber without any tectonic influence from the shallow magma chamber.

The example of Miyakejima suggests that the location, shape, and orientation of a shallow magma chamber will control the orientation and propagation direction of the feeder dikes. Similar cases where the stress of a magma plumbing system influence dike propagation are recognized in several basaltic volcanoes (e.g., Stromboli: Corazzato et al., 2008). The effect of local stress generated by an additional intrusion can be temporal because the stress relaxation weakens the local stress field in the host rock. The timescale of the stress relaxation is, in general, difficult to evaluate because it depends on the macroscopic viscoelastic behavior of the volcanic edifice which is controlled by the mechanical and thermal structure and the magnitude of the local stress field. Some field observations can suggest the time scale; in the case of Fernandina volcano, the local stress field generated by the emplacement of a sill in 1995 can remain and control the development of the eruption fissure of 2005 (Bagnardi et al., 2013). The local distribution of the eruption fissures may suggest frequent intrusions with a relatively short interval as the case of Miyakejima (2–3 events per 100 years).

The propagation direction of dikes in a volcanic edifice can be also affected by the topographic contrast, especially in an asymmetric edifice (e.g., Tibaldi et al., 2014; Corbi et al., 2015; Rivalta et al., 2015 and references therein).The volcanic edifice of Miyakejima, including its submarine part, has a conical shape without any remarkable bulge along the rift zone (**Figure 1B**). The development of the NE-SW rift zone became significant within the last 2800 years. However, no remarkable change in the shape of the edifice was noted in this period. These facts suggest that the topographic control on the rift development is limited in the case of Miyakejima.

FIGURE 4 | (A) Illustration of the definition of the offset angle of an eruption fissure. (B) Whole-rock SiO$_2$ content of the ejecta from the flank eruption fissures during the last 2800 years plotted against the offset angle of their eruption fissure.

FIGURE 5 | Schematic model of the magma plumbing system of Miyakejima. (A) A basaltic dike extending from the from the deep-seated basaltic magma chamber injected into the shallow magma chamber filled with andesitic magma. Injection causes magma mixing within the shallow magma chamber and a dike with hybrid magma propagates from the shallow magma chamber. Injection also causes the rapid increase of the internal magma pressure in the shallow magma chamber to a local stress field around the shallow chamber. Orientation of the dike from the shallow magma chamber is mainly controlled by the local stress field generated by the pressurized shallow magma chamber. (B) A basaltic dike propagates directly from the deep-seated magma chamber without intersecting the shallow magma chamber. The orientation of the eruption fissure is mainly controlled by the regional stress field.

CONCLUSIONS

Combined analyses of the distribution patterns of the eruption fissures and the magmatic composition of the lavas within the last ∼2800 years reveal that a shallow andesitic magma chamber beneath the summit of Miyakejima volcano controls the orientation of eruption fissures. The injection of basaltic magma into the shallow andesitic magma chamber caused a rapid increase in the internal magmatic pressure in this magma chamber. The local compressive stress field around the andesitic magma chamber controls the orientation of feeder dikes in the NE-SW rift zone. Development of the NE-SW rift zone after a

major eruption in the ninth century indicates that the shallow magma chamber is a remnant magma chamber formed during the ninth century eruption.

AUTHOR CONTRIBUTIONS

NG and TO prepares all the field data. NG did the petrological analysis. Reconstruction of the eruption history is mainly by TO. NG and TO build the manuscript.

REFERENCES

Amma-Miyasaka, M., and Nakagawa, M. (2003). Evolution of deeper basaltic and shallower andesitic magmas during the ad 1469–1983 eruptions of Miyake-Jima Volcano, Izu– Mariana Arc: inferences from temporal variations of mineral compositions in crystal-clots. *J. Petrol.* 44, 2113–2138. doi: 10.1093/petrology/egg072

Amma-Miyasaka, M., Nakagawa, M., and Nakada, S. (2005). Magma plumbing system of the 2000 eruption of Miyakejima Volcano, Japan. *Bull. Volcanol.* 67, 254–267. doi: 10.1007/s00445-004-0408-0

Aramaki, S., Hayakawa, Y., Fujii, T., Nakamura, K., and Fukuoka, T. (1986). The October 1983 eruption of Miyakejima volcano. *J. Volcanol. Geotherm. Res.* 29, 203–229. doi: 10.1016/0377-0273(86)90045-4

Bagnardi, M., Amelung, F., and Poland, M. P. (2013). A new model for the growth of basaltic shields based on deformation of Fernandina volcano, Galápagos Islands. *Earth Planet. Sci. Lett.*, 377–378, 358–366. doi: 10.1016/j.epsl.2013.07.016

Cappello, A., Geshi, N., Neri, M., and Del Negro, N. (2015). Lava flow hazards – An impending threat at Miyakejima volcano, Japan. *J. Volcanol. Geotherm. Res.* 308, 1–9. doi: 10.1016/j.jvolgeores.2015.10.005

Chadwick, W. W., and Dieterich, J. H. (1995). Mechanical modeling of circumferential and radial dike intrusion on Galapagos volcanoes. *J. Volcanol. Geotherm. Res.* 66, 37–52. doi: 10.1016/0377-0273(94)00060-T

Chadwick, W. W., and Howard, K. A. (1991). The pattern of pattern of circumferential and radial eruptive fissures on the volcanoes of Fernandina and Isabela islands, Galapagos. *Bull. Volcanol.* 53, 259–275. doi: 10.1007/BF00414523

Chadwick, W. W., Jónsson, S., Geist, D. J., Poland, M., Johnson, D. J., Batt, S., et al. (2011). The May 2005 eruption of Fernandina volcano, Galápagos: The first circumferential dike intrusion observed by GPS and InSAR. *Bull. Volcanol.* 73, 679–697. doi: 10.1007/s00445-010-0433-0

Corazzato, C., Francalanci, L., Menna, M., Petrone, C., Renzulli, A., Tibaldi, A., et al. (2008). What does it guide sheet intrusion in volcanoes? Petrological and structural characters of the Stromboli sheet complex, Italy. *J. Volcanol. Geotherm. Res.* 173, 26–54. doi: 10.1016/j.jvolgeores.2008.01.006

Corbi, F., Rivalta, E., Pinel, V., Maccaferri, F., Bagnardi, M., and Acocella, V. (2015). How caldera collapse shapes the shallow emplacement and transfer of magma in active volcanoes. *Earth Planet Sci. Lett.* 431, 287–293. doi: 10.1016/j.epsl.2015.09.028

Falsaperla, S., and Neri, M. (2015). Seismic footprints of shallow dyke propagation at Etna, Italy. *Sci. Rep.* 5:11908. doi: 10.1038/srep11908

Geshi, N., Shimano, T., Nagai, M., and Nakada, S. (2002). Caldera collapse during the 2000 eruption of Miyakejima volcano, Japan. *Bull. Volcanol.* 64, 55–68. doi: 10.1007/s00445-001-0184-z

Gudmundsson, A. (2006). How local stresses control magma-chamber ruptures, dyke injections, and eruptions in composite volcanoes. *Earth Sci Rev.* 79, 1–31. doi: 10.1016/j.earscirev.2006.06.006

Irwan, M., Kimata, F., and Fujii, N. (2006). Time dependent modeling of magma intrusion during the early stage of the 2000 Miyakejima activity. *J. Volcanol. Geotherm. Res.* 150, 102–112. doi: 10.1016/j.jvolgeores.2005.07.014

Ishizuka, O., Geshi, N., Itoh, J., Kawanabe, Y., and TuZino, T. (2008). The magmatic plumbing of the submarine Hachijo NW volcanic chain, Hachijojima, Japan: long-distance magma transport? *J. Geophys. Res.* 113:B08S08. doi: 10.1029/2007jb005325

Ishizuka, O., Geshi, N., Kawanabe, Y., Ogitsu, I., Taylor, R. N., Tuzino, T., et al. (2014). Long-distance magma transport from arc volcanoes inferred from the submarine eruptive fissures offshore Izu-Oshima volcano, Izu–Bonin arc. *J. Volcanol. Geotherm. Res.* 285, 1–17. doi: 10.1016/j.jvolgeores.2014.08.006

Ito, T., and Yoshida, S. (2002). A dike intrusion model in and around Miyakejima, Niijima and Kozushima in 2000. *Tectonophy* 359, 171–187. doi: 10.1016/S0040-1951(02)00510-3

Kobayashi, T., Ohminato, T., Ida, Y., and Fujita, E. (2009). Very long period seismic signals observed before the caldera formation with the 2000 Miyake-jima volcanic activity, Japan. *J. Geophys. Res.* 114:B02211. doi: 10.1029/2007jb005557

Koyama, M., and Umino, S. (1991). Why does the Higashi-Izu monogenetic volcano group exist in the Izu Peninsula? Relationships between late Quaternary volcanism and tectonics in the northern tip of the Izu-Bonin arc. *J. Phys. Earth.* 39, 391–420. doi: 10.4294/jpe1952.39.391

Kumagai, H., Ohminato, T., Nakano, M., Ooi, M., Kubo, A., Inoue, H., et al. (2001). Very-long-period seismic signals and caldera formation at Miyake Island, Japan, *Science* 293, 687–690. doi: 10.1126/science.1062136

Kuritani, T., Yokoyama, T., Kobayashi, K., and Nakamura, E. (2003). Shift and rotation of composition trends by magma mixing: 1983 Eruption at Miyake-jima Volcano, Japan. *J. Petrol.* 44, 1895–1916. doi: 10.1093/petrology/egg063

Letourneur, L., Peltier, A., Staudacher, T., and Gudmundsson, A. (2008). The effects of rock heterogeneities on dyke paths and asymmetric ground deformation: The example of Piton de la Fournaise (Réunion Island). *J. Volcanol. Geotherm. Res.* 173, 289–302. doi: 10.1016/j.jvolgeores.2008.01.018

Munekane, H., Oikawa, J., and Kobayashi, T. (2016). Mechanisms of step-like tilt changes and very long period seismic signals during the 2000 Miyakejima eruption: insights from kinematic GPS. *J. Geophy. Res. Solid Earth* 121, 2932–2946. doi: 10.1002/2016JB012795

Nakamura, K. (1977). Volcanoes as possible indicators of tectonic stress orientation — principle and proposal. *J. Volcanol. Geotherm. Res.* 2, 1–16. doi: 10.1016/0377-0273(77)90012-9

Nakano, S., and Yamamoto, T. (1991). Chemical variations of magmas at Izu–Oshima volcano, Japan: plagioclase-controlled and differentiated magmas. *Bull. Volcanol.* 53, 112–120. doi: 10.1007/BF00265416

Niihori, K., Tsukui, M., and Kawanabe, Y. (2003). Evolution of magma and magma plumbing system of Miyakejima Volcano in the last 10,000 years. *Bull. Volcanol. Soc. Japan* 48, 387–405.

Nishimura, T. (2011). Back-arc spreading of the northern Izu–Ogasawara (Bonin) Islands arc clarified by GPS data. *Tectonophy* 512, 60–67. doi: 10.1016/j.tecto.2011.09.022

Nishimura, T., Ozawa, S., Murakami, M., Sagiya, T., Tada, T., Kaizu, M., et al. (2001). Crustal deformation caused by magma migration in the northern Izu Islands, Japan. *Geophys. Res. Lett.* 28, 3745–3748. doi: 10.1029/2001GL013051

Ozawa, T., and Fujita, E. (2013). Local deformations around volcanoes associated with the 2011 off the Pacific coast of Tohoku earthquake. *J. Geophy. Res. Solid Earth* 118, 390–405. doi: 10.1029/2011JB009129

Rivalta, E., Taisne, B., Bunger, A., and Katz, R. (2015). A review of mechanical models of dike propagation: schools of thought, results and future directions. *Tectonophysics* 638, 1–42. doi: 10.1016/j.tecto.2014.10.003

Saito, G., Morishita, Y., and Shinohara, H. (2010). Magma plumbing system of the 2000 eruption of Miyakejima volcano, Japan, deduced from volatile and major component contents of olivine-hosted melt inclusions. *J. Geophys. Res.* 115:B11202. doi: 10.1029/2010jb007433

Saito, G., Uto, K., Kazahaya, K., Shinohara, H., Kawanabe, Y., and Satoh, H. (2005). Petrological characteristics and volatile content of magma from the 2000 eruption of Miyakejima Volcano, Japan. *Bull. Volcanol.* 67, 268–280. doi: 10.1007/s00445-004-0409-z

Seebeck, H., and Nicol, H. (2009). Dike intrusion and displacement accumulation at the intersection of the Okataina Volcanic Centre and Paeroa Fault zone, Taupo Rift, New Zealand. *Tectonophy* 475, 575–585. doi: 10.1016/j.tecto.2009.07.009

Takada, A. (1997). Cyclic flank-vent and central-vent eruption patterns. *Bull. Volcanol.* 58, 539–556. doi: 10.1007/s004450050161

Tibaldi, A. (2015). Structure of volcano plumbing systems: a review of multi-parametric effects. *J. Volcanol. Geotherm. Res.* 298, 85–135. doi: 10.1016/j.jvolgeores.2015.03.023

Tibaldi, A., Bonali, F. L., and Corazzato, C. (2014). The diverging volcanic rift system. *Tectonophy* 611, 94–113. doi: 10.1016/j.tecto.2013.11.023

Tsukui, M., Saito, K., and Hayashi, K. (2006). Frequent and intensive eruptions in the 9th century, Izu Islands, Japan: revisions of volcano-stratigraphy based on tephras and historical document. *Bul. Volcanol. Soc. Japan* 51, 327–338.

Tsukui, M., and Suzuki, Y. (1999). Eruptive history of Miyakejima Volcano during the last 7000 years. *Bull. Volcanol. Soc. Japan* 43, 149–166.

Ueda, H., Fujita, E., Ukawa, M., Yamamoto, E., Irwan, M., and Kimata, F. (2005). Magma intrusion and discharge process at the initial stage of the 2000 activity of Miyakejima, central Japan, inferred from tilt and GPS data. *Geophys. J. Int.* 161, 891–906. doi: 10.1111/j.1365-246X.2005.02602.x

Walter, T. R., Troll, V. R., Cailleau, B., Belousov, A., Schmincke, H.-U., Amelung, F., et al. (2005). Rift zone reorganization through flank instability in ocean island volcanoes: an example from Tenerife, Canary Islands. *Bull. Volcanol.* 67, 281–291. doi: 10.1007/s00445-004-0352-z

Yamaji, A., and Sato, K. (2011). Clustering of fracture orientations using a mixed Bingham distribution and its application to paleostress analysis from dike or vein orientations. *J. Struct. Geol.* 33, 1148–1157. doi: 10.1016/j.jsg.2011.05.006

Yamaoka, K., Kawamura, M., Kimata, F., Fujii, N., and Kudo, T. (2005). Dike intrusion associated with the 2000 eruption of Miyakejima Volcano, Japan. *Bull. Volcanol.* 67, 231–242. doi: 10.1007/s00445-004-0406-2